Gauge-invariant method for the $\pm J$ spin-glass model

J. A. Blackman

Department of Physics, University of Reading, Whiteknights, P.O. Box 220, Reading RG6 2AF, England

J. Poulter

Forum for Theoretical Science, Physics Department, Chulalongkorn University, Bangkok 10330, Thailand
(Received 24 September 1990; revised manuscript received 1 April 1991)

This paper deals with the $\pm J$ Ising model in two dimensions in the general case where there is a concentration p of negative bonds. We are particularly interested in exploring the Pfaffian (or combinatorial) method for treating this problem because a Green's-function formalism can be developed in which the frustration manifests itself in a gauge-invariant form through temperature-dependent singularities. We describe the formalism in detail and show how the disappearance of ferromagnetic order at a critical value of p can be related to a transition from localized to extended states analogous to the Anderson transition. Calculations are performed for the ground-state energy and entropy, which are obtained exactly for large samples. We introduce an exponent ρ that describes the underlying singularity structure of the Green's-function formalism and we show how this is related to the exponent of the spin-spin correlation function of the Ising problem. A value for this exponent of $\eta = 0.4$ is obtained.

I. INTRODUCTION

There have been a number of attempts to develop a theory for short-range spin glasses based on the gauge-invariant features of the system. Toulouse[1] introduced the concept of a frustrated plaquette as a gauge-invariant description of the element of disorder in a two-dimensional $\pm J$ model. Further studies, which aimed to exploit the gauge invariant aspects, were made by Fradkin, Huberman, and Shenker,[2] Kogut,[3] and Schuster.[4]

The subsequent developments, however, have been predominantly numerical, either via Monte Carlo simulations or the transfer matrix method[5−9] or through the domain-wall renormalization-group approach.[10−12] A fairly clear understanding of the equilibrium and non-equilibrium properties has emerged from this work and the effort now is being directed into attempts to build a microscopic picture of the low-temperature state of a spin glass.

The main emphasis[13−15] at present is in the direction of building a scaling theory for droplet excitations. This is a natural development from the domain-wall renormalization-group approach. For Stein *et al.*[13] the approach allows them to incorporate a percolative aspect into the problem though of a different nature to normal percolative ideas. Reviews of various aspects of spin-glass theory have been given by Binder and Young,[16] Van Hemmen and Morgenstern,[17] and Young.[18]

In the present paper we wish to return to the gauge-invariant properties of the system and develop a microscopic theory based on that. We consider specifically the $\pm J$ Ising model

$$H = -\sum_{\langle ij \rangle} J_{ij} \sigma_i \sigma_j , \qquad (1.1)$$

where the bond distribution is

$$P(J_{ij}) = p\delta(J_{ij}+J)+(1-p)\delta(J_{ij}-J) . \qquad (1.2)$$

Our discussion will concentrate entirely on the 2D system, although, in the conclusion, we shall point out that there is a possible route for developments in 3D.

The formalism we use is based on the combinatorial or Pfaffian method.[19,20] Preliminary results on the frustration problem have already been reported,[21−23] and the method has been used also in another context.[24] To make this paper self-contained, we give a brief review (Sec. II) of the formalism but refer the reader to the earlier references for full details. The method employed can take several guises: combinatorics,[19] Pfaffians,[20] Grassmann variables.[25,26] The essential point, however, is that the problem can be expressed in terms of the properties of an eigenvalue spectrum or, if we use the Grassmann algebra, it is a noninteracting field theory in anticommuting variables (or an interacting field theory in three dimensions).

The thermodynamic properties can be written in terms of a Green's-function formalism and, in this format, any frustration in the system manifests itself in a characteristic way through temperature-dependent singularities that collapse to a single degenerate value at zero temperature. This singularity structure is fully gauge invariant and provides a key to a new understanding of the physics of short-range frustrated systems.

As p in Eq. (1.2) is increased from zero, the ferromagnetic critical temperature T_c decreases and, at a critical concentration p_c, ferromagnetic order disappears ($T_c \rightarrow 0$). p_c is around 12–15%. The canonical $\pm J$ spin glass is at 50%.

We can examine the eigenstates associated with the singularity structure. It is found that, for $p < p_c$, all of them are localized. For $p > p_c$, extended states begin to appear. It is shown that the size distribution of the eigen-

states obeys a power law with an exponent ρ. There is a critical value ρ_c for this exponent which marks the transition from localized to extended states. It is argued that $\rho \rightarrow \rho_c$ as $p \rightarrow p_c$. Thus, although as was shown[27] a number of years ago, there is no thermodynamic fixed point at p_c, there is a quantity that goes through a critical value at this concentration.

In this paper, we use the formalism to calculate thermodynamic quantities: the ground-state free energy and entropy at $p = 50\%$ and also the exponent of the correlation function at this concentration. Its purpose, however, is also to provide a language for describing the physics of short-range frustrated systems.

The outline of this paper is as follows. After a review of the formalism in Sec. II, we analyze in Sec. III the singularity structure, which, it has been asserted, contains the gauge-invariant characteristics of the frustrated system. In Sec. IV an expression for the ground-state entropy is developed within this formalism. Numerical calculations on large samples are effected by degenerate-state perturbation theory—typically with a degeneracy of several thousand and a perturbation expansion to between 7th and 13th order. The perturbation theory is developed in Sec. V. It is to be emphasized that perturbation theory in this context is not to be regarded as an approximation. Rather, it is a systematic expansion that is exact if taken to high enough order.

In Sec. VI, the ground-state energy and entropy at $p = 50\%$ are calculated numerically with results that we claim are the most accurate available in the literature. We have remarked that p_c is marked by a transition from localized to extended states (a sort of Anderson transition). There is an exponent ρ that describes the spatial extent of the states. This is calculated for two values of concentration in the $p < p_c$ regime, and it is shown that $\rho > \rho_c$, where ρ_c is the value of the exponent at the localized-extended transition. Finally, in Sec. VIII, we consider the concentration $p = 50\%$. The spatial distribution of the eigenstates associated with the singularity structure is again investigated. In this case it is found that the exponent ρ is smaller than the critical value ρ_c and the states are extended. It is shown that, for extended states, the exponent is related to that of the spin-spin correlation function and a value for the exponent of the correlation function is deduced.

II. THE PFAFFIAN FORMALISM FOR A DISORDERED SYSTEM

In the Pfaffian method[21] we write the partition function for the $2D$ Ising model as

$$Z = 2^N \left[\prod_{\langle ij \rangle} \cosh(J_{ij}/kT) \right] (\det D)^{1/2} , \qquad (2.1)$$

where J_{ij} is the nearest-neighbor bond strength for sites $\langle ij \rangle$ and the product is over all bonds on the N-site lattice. The matrix D is Hermitian, pure imaginary, and of order $4N$. D is more often written [19,20] in a real skew-symmetric form, but multiplying each element of the skew-symmetric array by i does not alter the result and we find it convenient to work with a matrix with real ei-

genvalues. We can also write Eq. (2.1) in terms of an integral over $4N$ Grassmann variables η, because

$$(\det D)^{1/2} = \int d\eta \exp \left[\frac{1}{2} \sum_{\alpha, \beta} \eta_\alpha D_{\alpha\beta} \eta_\beta \right] , \qquad (2.2)$$

although we shall not make use of this form in the present paper. The Grassmann formalism is necessary for developments in $3D$.

To display the form of D it is convenient to associate four nodes (labeled 1–4) with each site of the lattice as in Fig. 1 (the notation used is as in Ref. 24). D contains N blocks Ω down the diagonal; the elements of each block connect nodes associated with a single lattice site

$$\Omega = \begin{bmatrix} 0 & -i & i & i \\ i & 0 & -i & i \\ -i & i & 0 & -i \\ -i & -i & i & 0 \end{bmatrix} . \qquad (2.3)$$

D also contains matrix elements that link nodes 1 (3) of one site with 2 (4) of neighboring sites along the x (y) Cartesian directions. These correspond to the bonds J_{ij} connecting sites i and j, and the elements in D are equal to $\mp i t_{ij}$ where $t_{ij} = \tanh(J_{ij}/kT)$. The minus and plus signs correspond, respectively, to the positive and negative Cartesian directions. Ω is independent both of temperature and any disorder in the system. These enter only through t_{ij}.

For a perfect system at zero temperature, the eigenvalues ϵ of D lie in a band such that $2 - \sqrt{2} \leq |\epsilon| \leq 2 + \sqrt{2}$. The eigenvalues occur in pairs at $\pm \epsilon$. At the critical temperature T_c there is a pair of eigenvalues at $\epsilon = 0$ (zero mass gap).

A single negative defect in an otherwise perfect lattice produces a pair of frustrated plaquettes. It also produces a pair of defect eigenvalues that approach 0 in the zero T limit as $\epsilon = \pm \frac{1}{2} \exp(-2J/kT)$. These defect eigenstates are localized on the frustrated plaquettes at $T = 0$.

In the presence of an arbitrary number of negative bonds, a band of defect eigenstates is produced. These eigenstates are equal in number to the number of frustrat-
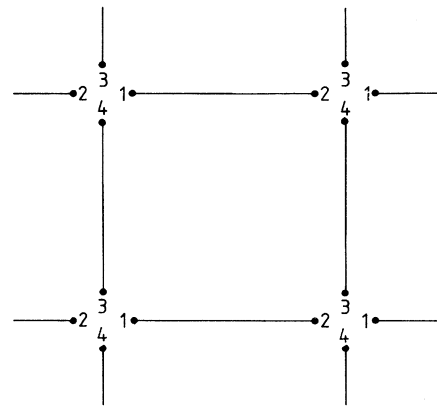
FIG. 1. The labeling of nodes associated with a lattice site.

ed plaquettes and, as in the case of a single defect, are completely localized on the frustrated plaquettes at zero temperature. Each eigenvalue can be written

$$\epsilon = \pm \tfrac{1}{2} X \exp(-2Jr/kT) , \tag{2.4}$$

where r is an integer and X is a real number. At $T=0$ there is a degeneracy at $\epsilon = 0$ equal to the number of frustrated plaquettes. Because of the one-to-one correspondence with the frustrated plaquettes, the eigenstates characterized by Eq. (2.4) form the basis for a gauge-invariant development.

We stated earlier[22] that the change in the ground-state energy and entropy of the system that results from the introduction of frustration can be written

$$\Delta F = 2J \sum_d{}^+ r_d , \tag{2.5}$$

$$\Delta S = k \sum_d{}^+ \ln X_d , \tag{2.6}$$

where the notation indicates a summation of positive eigenstates of Eq. (2.4). Equations (2.5) and (2.6) are the gauge-invariant expressions for the two fundamental ground-state properties based as they are on quantities firmly related to the spatial distribution of frustrated plaquettes. Equation (2.6) is, of course, equivalent to expressing the ground-state degeneracy M as

$$M = \prod_d{}^+ X_d . \tag{2.7}$$

These key ground-state results were first quoted in Ref. 22. Although the derivation of Eq. (2.5) is almost trivial, that of Eq. (2.6) is quite subtle. The proof comes via a Green's-function approach, which follows in the next two sections.

There is an apparent similarity in our formalism to Toulouse's[1] string description of the ground state in which frustrated plaquettes are connected in pairs in such a way as to minimize the total string length. It is important to realize, however, that our approach and the string formalism are quite distinct. This is best illustrated by
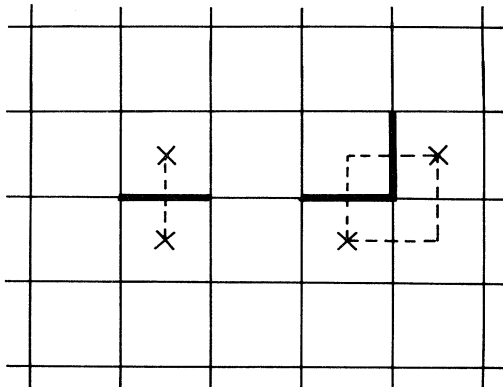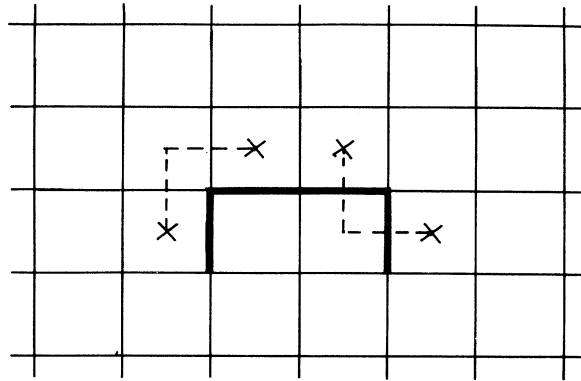
FIG. 3. A more complex defect configuration with one of the five possible minimum string-length configurations drawn. Heavy lines denote negative bonds.

means of an example. Two elementary defect configurations are shown in Fig. 2. In the first (on the left), the string connecting the pair of frustrated plaquettes is of unit length signifying one wrong bond. In the second (on the right) a string of two units of length can be drawn in two ways, indicating two wrong bonds and a doubly degenerate ground state. In the present formalism the frustration would manifest itself in a pair of defect eigenstates of the form of Eq. (2.4) with $X=1$, $r=1$ for the first configuration and $X=2$, $r=2$ for the second.

In Fig. 3, a slightly more complex configuration is shown. Strings with a total length of four units are drawn, indicating four wrong bonds. There are five ways of drawing this consistent with a fivefold degenerate ground state. In our formalism, because of the presence of four frustrated plaquettes, there are two pairs of defect eigenstates of the form of Eq. (2.4). One has $X=1$, $r=1$, while the values for the other are $X=5$, $r=3$, giving four $(3+1)$ wrong bonds and a degeneracy of five (5×1).

The string picture provides a description of the ground state, but is not a practical method of determining the ground-state properties because there is no methodology (other than by inspection) for obtaining all the minimum string-length configurations. Our formalism does not attempt to determine the ground-state configurations themselves. Rather, by matrix diagonalization, a set of values for X and r is obtained, from which the energy and entropy can be determined. The approach is completely gauge invariant and depends solely on the number of frustrated plaquettes and their spatial distribution.

III. SINGULARITY STRUCTURE OF THE ZERO-TEMPERATURE T MATRIX

As was stated in the introduction, $\det D$ in Eq. (2.1) is a gauge-invariant quantity and, at zero temperature, the frustration manifests itself in a gauge-invariant way through the zeros of D. It is convenient to express the formalism in the language of resolvent Green's functions,

FIG. 2. Two simple defect configurations. Minimum string-length configurations are shown according to the Toulouse (Ref. 1) description. Heavy lines denote negative bonds.

where, as we shall show, the frustration appears as separable singularities. The Green's function for the problem is defined by

$$G = (\epsilon I - D)^{-1} , \tag{3.1}$$

where ϵ is a real dimensionless quantity whose purpose is essentially one of accounting and I is the $4N \times 4N$ unit matrix.

The matrix D can be expressed as

$$D = D_0 + V , \tag{3.2}$$

where D_0 is the corresponding matrix for the perfect crystal [i.e., J_{ij} equal to a constant value J in Eq. (1.1)], and V is the perturbation describing the defect distribution. The associated T matrix is given by

$$T = V(I - gV)^{-1} , \tag{3.3}$$

where g is the Green's function of the perfect lattice.

The basis of the matrix D is usually given by four nodes at each lattice site, as shown in Fig. 1. However, in order to facilitate the development of the formalism, it is useful to introduce a fresh basis more obviously associated with bonds and plaquettes, as shown in Fig. 4. The basis is given by

$$|\pm\rangle = 2^{-1/2}(|\alpha\rangle \pm |\beta\rangle) , \tag{3.4}$$

where $|\alpha\rangle$ and $|\beta\rangle$ are in the original node basis.

The perfect-crystal Green's function g_0 [$= g(\epsilon = 0)$] can be calculated[24] by transforming D_0 into a plane-wave basis and inverting a 4×4 matrix. For zero temperature, g_0 is highly localized. Its only nonzero elements are across a single bond

$$g_0(+, -) = -g_0(-, +) = -\tfrac{1}{2}i \tag{3.5}$$

and within a plaquette

$$g_0 = \tfrac{1}{2} \begin{bmatrix} 0 & i & i & i \\ -i & 0 & -i & -i \\ -i & i & 0 & -i \\ -i & i & i & 0 \end{bmatrix} , \tag{3.6}$$
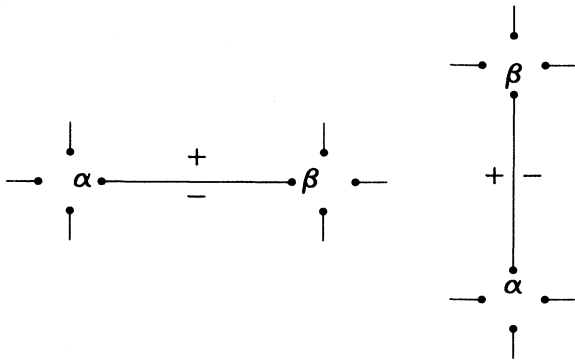
where the elements of g_0 in Eq. (3.6) are with respect to the bond basis of a plaquette (see Fig. 5).

We now consider the $\pm J$ problem [Eq. (1.2)] specifically. A defect basis can be defined in terms of all the states $|\pm\rangle$ associated with the negative bonds. Both the perturbation V and the T matrix are expressed in terms of this defect basis. In particular,

$$V(+, -) = -V(-, +) = -2i \tag{3.7}$$

across a negative bond for zero temperature. All other elements of V are zero. From Eq. (3.7) it follows that $V^{-1} = \tfrac{1}{4}V$, and so the inverse of the T matrix is given by

$$T^{-1} = \tfrac{1}{4}V - g . \tag{3.8}$$

In general negative bonds may be placed at any position at random. However, it is convenient, after positioning the negative bonds, to perform a series of gauge transformations in order that all the defect bonds are, say, vertical. This reduces the complexity of the problem. After these transformations any plaquette is one of four types, as in Fig. 6. There are two types of unfrustrated plaquettes and two types that are frustrated. Note that gauge transformations never change the distribution of frustrated plaquettes or the partition function of the lattice.

The defect subspace of the gauge-transformed system is generally of a different size to that of the system prior to the gauge transformation, but since we are interested in gauge-invariant properties this is immaterial. We choose a gauge that is convenient for the development of the formalism.

We consider first T^{-1} of Eq. (3.8) in the $\epsilon = 0$ limit. It is useful to regard the defect basis states as being of two types depending on whether the plaquette they are in is frustrated or not. If a state is within a frustrated plaquette it will be written $|f\rangle$, and otherwise $|u\rangle$, and let us suppose that there are a total of n and n' states, respectively, of each type in the lattice. Across any defect bond it is evident from Eqs. (3.5) and (3.7) that

FIG. 4. The transformation from a node to a bond basis.
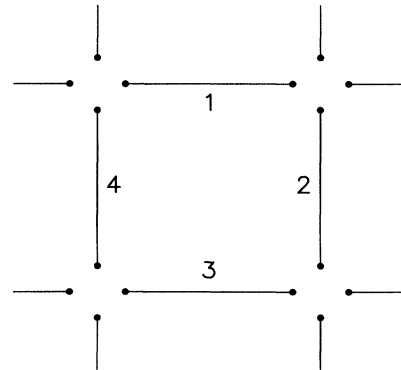
FIG. 5. The states in a bond basis associated with a single plaquette. Those numbered 2 and 3 are of type $|+\rangle$ and those numbered 1 and 4 are of type $|-\rangle$.
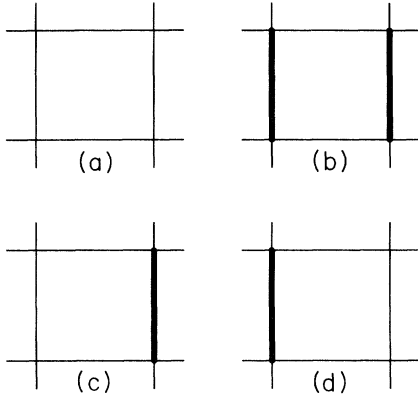
FIG. 6. Possible plaquettes after gauge transformation to vertical defect bonds (indicated by heavy lines). Plaquettes (a) and (b) are unfrustrated while (c) and (d) are frustrated. There are no defect states in (a); there are two of type $|u\rangle$ in (b) and one of type $|f\rangle$ in each of (c) and (d).

$\frac{1}{4}V(+,-)-g_0(+,-)=0$. From this it can be seen that any matrix elements of T^{-1} involving an $|f\rangle$ are zero and the only nonzero elements are those between the unfrustrated defect states $|u\rangle$ within a plaquette of type (b) in Fig. 6. Let us define the matrix U by

$$U^{-1}=\sum_{u,u'}|u\rangle\langle u|(\tfrac{1}{4}V-g_0)|u'\rangle\langle u'| . \tag{3.9}$$

Then we can write

$$\tfrac{1}{4}V-g_0=\begin{bmatrix}0 & 0\\ 0 & U^{-1}\end{bmatrix} , \tag{3.10}$$

where the upper (lower) blocks of order $n\,(n')$ are associated with frustrated (unfrustrated) states and the singularities in $T(\epsilon=0)$ are clearly seen to be associated with the frustrated plaquettes. The matrix U has nonzero elements only within an unfrustrated plaquette with two defects (second diagram of Fig. 6). Within such a plaquette,

$$U(+,-)=-U(-,+)=2i , \tag{3.11}$$

and the diagonal elements are zero.

To obtain g, we treat ϵ as a small parameter and expand

$$g=g_0-\epsilon g_0^2+\epsilon^2 g_0^3+O(\epsilon^3) , \tag{3.12}$$

so that

$$T^{-1}=(\tfrac{1}{4}V-g_0)+\epsilon g_0^2-\epsilon^2 g_0^3+O(\epsilon^3) . \tag{3.13}$$

A useful simplification in the inversion of Eq. (3.13) is the relation

$$\langle f|g_0^2|f'\rangle=\langle f|f'\rangle , \tag{3.14}$$

which follows from Eqs. (3.5) and (3.6). This enables us to write

$$T=\begin{bmatrix}\epsilon^{-1}I & 0\\ 0 & 0\end{bmatrix}+\begin{bmatrix}QUQ^{\dagger}+C & -QU\\ -UQ^{\dagger} & U\end{bmatrix}+O(\epsilon) , \tag{3.15}$$

where

$$Q=\sum_{fu}|f\rangle\langle f|g_0^2|u\rangle\langle u| \tag{3.16}$$

and

$$C=\sum_{ff'}|f\rangle\langle f|g_0^3|f'\rangle\langle f'| . \tag{3.17}$$

I is the unit matrix with dimensions equal to the number n of frustrated plaquettes.

To emphasize the separation of the singular behavior associated with the frustration, let us reexpress Eq. (3.15) as

$$T=\epsilon^{-1}\sum_f|f\rangle\langle f|+S+O(\epsilon) , \tag{3.18}$$

where S is the second term in Eq. (3.15). Eqs. (3.15) and (3.18) are the key results of this section.

IV. THE GROUND-STATE ENTROPY

The ground-state energy of the system has been expressed in Eq. (2.5) in terms of the quantity r_d in the exponent of the defect eigenvalues of Eq. (2.4). We will show here how the corresponding entropy can be related to X_d from the same expression to give Eq. (2.6). For the $\pm J$ problem, the partition function, from Eq. (2.1), can be written

$$\frac{Z}{Z_0}=\left[\frac{\det D}{\det D_0}\right]^{1/2} , \tag{4.1}$$

where the subscript 0 refers to the perfect system. Let us denote the eigenvalues of D_0 by ϵ_p and those of D by ϵ_d [the defect eigenvalues of Eq. (2.4)] or ϵ_c (the remaining continuum ones). Then

$$\frac{\det D}{\det D_0}=\frac{\prod_c\epsilon_c\prod_d\epsilon_d}{\prod_p\epsilon_p} . \tag{4.2}$$

It will be shown that the ratio of the products of ϵ_c and ϵ_p is a pure number independent of the disorder in the system so that the effects of frustration are entirely described by the ϵ_d.

Consider the Green's function defined in Eq. (3.1). It can be written, at zero temperature, in terms of the defect and continuum eigenstates as

$$G=\sum_c|c\rangle(\epsilon-\epsilon_c)^{-1}\langle c|+\epsilon^{-1}\sum_d|d\rangle\langle d| , \tag{4.3}$$

so that in the limit $\epsilon\to0$

$$\det G=\epsilon^{-n}\left[\prod_c\epsilon_c\right]^{-1} , \tag{4.4}$$

where n is the total number of frustrated plaquettes. A minus sign is unnecessary on ϵ_c in Eq. (4.4) because all states occur in positive and negative pairs. Now from the relation $G=(I-gV)^{-1}g$, we can write

$$\det G=\det g/\det(I-gV) . \tag{4.5}$$

But the determinant of $I - gV$ is the same whether evaluated in the defect basis only or in the full $4N \times 4N$ basis. The T matrix in Eq. (3.3) is in the defect basis and so it follows that

$$\det G / \det g = \det T / \det V ,\qquad (4.6)$$

and, from Eq. (3.15), to leading order in ϵ^{-1}

$$\det T = \epsilon^{-n} \det U .\qquad (4.7)$$

Now $\det g$ is, of course, equal to $\prod_p \epsilon_p^{-1}$ and so, from Eqs (4.4), (4.6), and (4.7), we can write

$$\frac{\prod_c \epsilon_c}{\prod_p \epsilon_p} = \frac{\det V}{\det U} .\qquad (4.8)$$

For k defect bonds $\det V = (-4)^k$, and for l unfrustrated plaquettes with two defects $\det U = (-4)^l$. Therefore, since $k - 1 = n/2$, the ratio in Eq. (4.8) is equal to $(-4)^{n/2}$ and, from Eq. (4.2),

$$\frac{\det D}{\det D_0} = (-4)^{n/2} \prod_d (\epsilon_d) .\qquad (4.9)$$

The eigenvalues of D have a symmetric distribution about zero and thus, from Eqs. (2.4) and (4.1), we can write

$$Z / Z_0 = 2^{n/2} \prod_d {}^+ \epsilon_d = \prod_d {}^+ X_d \exp(-2Jr_d/kT) ,\qquad (4.10)$$

where the notation indicates that the product is taken over only the positive eigenvalues. Thus the free energy in the limit $T \to 0$ limit is given by

$$F = F_0 - kT \sum_d {}^+ \ln X_d + 2J \sum_d {}^+ r_d ,\qquad (4.11)$$

where F_0 is the free energy of the perfect system. Thus the changes in the ground-state energy and entropy brought about by the introduction of frustration into the system are

$$\Delta F = 2J \sum_d {}^+ r_d ,\qquad (4.12)$$

$$\Delta S = k \sum_d {}^+ \ln X_d .\qquad (4.13)$$

It is worth emphasizing that the result of Eq. (4.13) is somewhat more subtle than that of Eq. (4.12). The contributions to Eq. (4.12) come entirely from the defect eigenstates. In Eq. (4.13) *precisely half* comes from the defect eigenstates. The remaining half arises from modifications to the continuum due to the introduction of frustration into the system. It is for this reason that X_d appears in Eq. (4.13) but only $\frac{1}{2} X_d$ in Eq. (2.4).

Equations (4.12) and (4.13) can be expressed equivalently in terms of the number of unsatisfied bonds N_w and the ground-state degeneracy M:

$$N_w = \sum_d {}^+ r_d ,\qquad (4.14)$$

$$M = \prod_d {}^+ X_d .\qquad (4.15)$$

V. DEGENERATE-STATE PERTURBATION THEORY

At zero temperature, the defect eigenstates are degenerate with value zero. To determine r_d and X_d we consider small finite temperature and use perturbation theory to lift the degeneracy. For finite temperatures the matrix D for the frustrated system is given by

$$D = D(0) + \delta D_1 ,\qquad (5.1)$$

where $D(0)$ is the matrix for the frustrated system at zero temperature and $\delta = 1 - \tanh J/kT$. Equation (5.1) is exact, but at low temperatures it is also convenient to use δ as a small parameter for a perturbation expansion.

We write the ground-state defect eigenstates in the form $|r, i\rangle$, where r is an integer representing the order of perturbation theory at which the degeneracy is lifted. It is also the index r in Eq. (2.4). i is a secondary index which labels the eigenstates of order r. Let $N(r)$ be the number of such eigenstates.

Our eigenvalue equation is

$$D|\Psi\rangle = \lambda |\Psi\rangle ,\qquad (5.2)$$

where λ is, say, the jth eigenvalue of order n,

$$\lambda = \delta^n \epsilon_n^j + O(\delta^{n+1}) .\qquad (5.3)$$

The eigenstate $|\Psi\rangle$ can be expanded in powers of δ,

$$|\Psi\rangle = |\Psi_0\rangle + \delta |\Psi_1\rangle + \delta^2 |\Psi_2\rangle + \cdots ,\qquad (5.4)$$

with $|\Psi_0\rangle \equiv |n, j\rangle$.

Equating powers of δ in Eqs. (5.2) to (5.4) we obtain (for $1 \leq m \leq n$)

$$D(0)|\Psi_m\rangle + D_1 |\Psi_{m-1}\rangle = \delta_{mn} \epsilon_n^j |n, j\rangle .\qquad (5.5)$$

By definition, $D(0)|r, i\rangle = 0$, so that

$$\langle r, i | D_1 | \Psi_{m-1}\rangle = \delta_{mn} \delta_{rn} \delta_{ij} \epsilon_n^j ,\qquad (5.6)$$

and, in particular, with $r = m = n = 1$,

$$\langle 1, i | D_1 | 1, j\rangle = \epsilon_1^j \delta_{ij} ,\qquad (5.7)$$

which is the expression that determines the eigenstates whose degeneracy is lifted at first order in δ [i.e., the $r = 1$ states in Eq. (2.4)].

Now, acting with a continuum state on Eq. (5.5), we have

$$\epsilon_c \langle c | \Psi_m\rangle = -\langle c | D_1 | \Psi_{m-1}\rangle .\qquad (5.8)$$

Then using closure

$$\sum_{r,i} |r, i\rangle \langle r, i| + \sum_c |c\rangle \langle c| = 1 ,\qquad (5.9)$$

and the definition of the continuum Green's function in Eq. (A1), we obtain

$$|\Psi_m\rangle = G_c D_1 |\Psi_{m-1}\rangle + \sum_{r=1}^{r_{max}} \sum_{i=1}^{N(r)} Z_r'^i |r, i\rangle ,\qquad (5.10)$$

where r_{max} is the highest order of perturbation theory required. $Z_r'^i$ is equal to $\langle r, i | \Psi_m\rangle$, but for our purposes these are just coefficients to be determined. Now, using

Eqs. (A7) and (5.6), we can write, in terms of a new set of coefficients Z_r^i,

$$|\Psi_m\rangle = g_c D_1 |\Psi_{m-1}\rangle - \delta_{mn} g_c \epsilon_n^j |n,j\rangle$$

$$+ \sum_{r=1}^{r_{max}} \sum_{i=1}^{N(r)} Z_r^i |r,i\rangle . \qquad (5.11)$$

Equations (5.6) and (5.11) are the key equations for the development to higher orders. To evaluate an eigenstate of order n, we need to consider values of m in Eq. (5.11) such that $1 \leq m \leq n-1$. Acting on Eq. (5.11) with $\langle r,i|D_1$ and using Eq. (5.6), we obtain

$$\delta_{m,n-1}\delta_{rn}\delta_{ij}\epsilon_n^j = \langle r,i|D_2|\Psi_{m-1}\rangle + \delta_{r1}Z_1^i\epsilon_1^i , \qquad (5.12)$$

where

$$D_2 = D_1 g_c D_1 . \qquad (5.13)$$

With $r = n = 2$ and $m = 1$, we obtain

$$\epsilon_2^j \delta_{ij} = \langle 2,i|D_1 g_c D_1|2,j\rangle , \qquad (5.14)$$

which yields the second-order states. For states of higher order than 2, inserting $r = 1$ in Eq. (5.12), gives

$$Z_1^i = -\langle 1,i|D_2|\Psi_{m-1}\rangle / \epsilon_1^i$$

and hence, from Eq. (5.11),

$$|\Psi_m\rangle = (1+G_1 D_1)g_c D_1|\Psi_{m-1}\rangle + \sum_{r=2}^{r_{max}} \sum_{i=1}^{N(r)} Z_r^i |r,i\rangle , \qquad (5.15)$$

where G_1 is a first-order Green's function, which is a special case of the definition

$$G_r = -\sum_{i=1}^{N(r)} |r,i\rangle (1/\epsilon_r^i)\langle r,i| . \qquad (5.16)$$

From Eq. (5.12), with $r \geq 3$, we obtain

$$\langle r,i|D_2|\Psi_{m-1}\rangle = \delta_{m,n-1}\delta_{rn}\delta_{ij}\epsilon_n^j . \qquad (5.17)$$

A similar procedure is now followed for the next order. Equation (5.15) is acted on with $\langle r,i|D_2$, which, using Eq. (5.17), gives

$$\delta_{m,n-2}\delta_{rn}\delta_{ij}\epsilon_n^j = \langle r,i|D_3|\Psi_{m-1}\rangle + \delta_{r2}Z_2^i\epsilon_2^i , \qquad (5.18)$$

where

$$D_3 = D_2(1+G_1 D_1)g_c D_1 . \qquad (5.19)$$

With $r = n = 3$ and $m = 1$, we obtain

$$\epsilon_3^j \delta_{ij} = \langle 3,i|D_3|3,j\rangle . \qquad (5.20)$$

Then setting $r = 2$ in Eq. (5.18) gives a value for Z_2^i which, inserting into Eq. (5.15), yields

$$|\Psi_m\rangle = (1+G_2 D_2)(1+G_1 D_1)g_c D_1|\Psi_{m-1}\rangle$$

$$+ \sum_{r=3}^{r_{max}} \sum_{i=1}^{N(r)} Z_r^i |r,i\rangle , \qquad (5.21)$$

while setting $r \geq 4$ in Eq. (5.18) gives

$$\langle r,i|D_3|\Psi_{m-1}\rangle = \delta_{m,n-2}\delta_{rn}\delta_{ij}\epsilon_n^j . \qquad (5.22)$$

The general rule is now apparent. The defect eigenvalues ϵ_r^i and the corresponding eigenvectors $|r,i\rangle$ are given by

$$\epsilon_r^j \delta_{ij} = \langle r,i|D_r|r,j\rangle , \qquad (5.23)$$

where, for $r > 1$, the hierarchy for D_r is obtained from

$$D_r = D_{r-1}(1+G_{r-2}D_{r-2})\cdots(1+G_1 D_1)g_c D_1 . \qquad (5.24)$$

VI. GROUND-STATE PROPERTIES AT $p = 50\%$

We now use the formalism of the previous section to calculate ΔF and ΔS numerically for large samples. A set of eigenvectors for the degenerate $\epsilon = 0$ state in the presence of an arbitrary amount of frustration is obtained easily by inspection. For small finite T the degeneracy is lifted and the X_d and r_d can be determined using Eqs. (5.7), (5.14), (5.20), and (5.23). We are using perturbation theory with δ as the small parameter as described in Sec. V; r_d is the order of perturbation theory at which the degeneracy is lifted. It is possible to go to sufficient orders that the degeneracy is lifted for all states and ΔF and ΔS are determined *exactly*. For a 128×128 sample, for example, the degeneracy at $T = 0$ is typically about 8000 and an expansion to between 7th and 13th order is necessary—but sufficient.

The ground-state energy and entropy at $p = 50\%$ have been calculated by several authors. The calculations we report here are, we believe, the most accurate so far performed. The numerical work was done on square samples of size L for a range of values of L up to 256. The
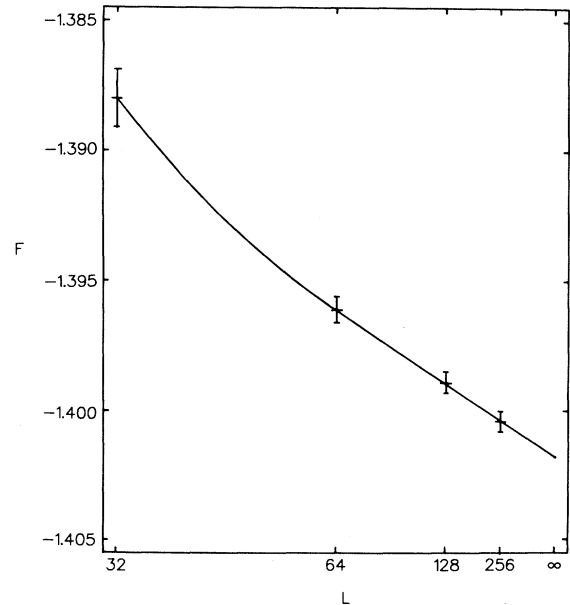
FIG. 7. Ground-state energy per site (in units of J) for square samples with sides of L sites for $p = 50\%$.
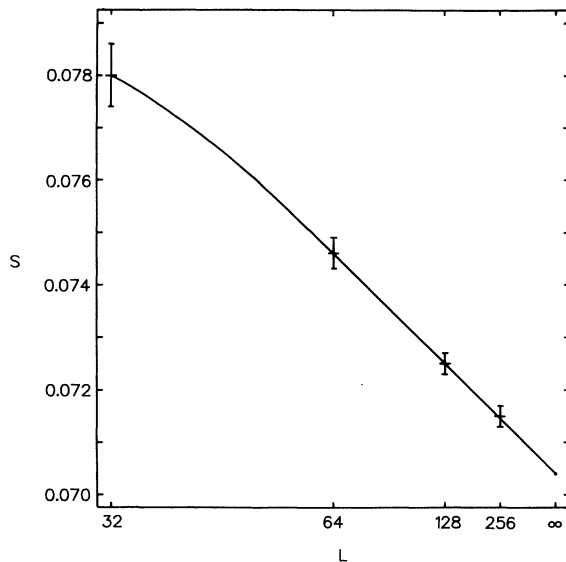
FIG. 8. Ground-state entropy per site (in units of k) of square samples of side L for $p = 50\%$.

samples were embedded in an essentially infinite unfrustrated background. In practice this means an unfrustrated frame to the sample of thickness equal to the order of perturbation theory to which it is necessary to go. Performing the degenerate-state perturbation theory on a sample with periodic boundary conditions would have been considerably more complex. Also we wished to avoid underestimating the effect of frustration by giving it the possibility of dissipating itself at free boundaries. There is a danger that our embedding method could overestimate the effect of frustration on the ground-state properties and so it was essential to perform calculations with a range of L values and extrapolate to infinity.

The results for the energy are shown in Fig. 7 and for the entropy in Fig. 8. The $L = 32$ and 64 results have been averaged over 200 samples. Those for $L = 128$ and 256 have been averaged over 80 and 40 samples, respectively. Error bars are shown in the diagrams. A linear extrapolation to infinity gives, for the ground-state energy and entropy per spin,

$$F = -1.4020 \pm 0.0004 \qquad (6.1)$$

TABLE I. Summary of previous values for the energy and entropy.

Reference	F	S
28	-1.39	0.099
29	-1.4	0.07
5	-1.4 ± 0.01	0.075
30	-1.4033	
6	-1.4024 ± 0.0012	0.0701 ± 0.0005
9	-1.407 ± 0.008	0.071 ± 0.007
a	-1.4020 ± 0.0004	0.0704 ± 0.0002

[a]Present work.

and

$$S = 0.0704 \pm 0.0002 . \qquad (6.2)$$

For comparison we tabulate results quoted by other authors (listed in chronological order of publication) (see Table I). Those by Cheung and McMillan[6] and by Wang and Swendsen[9] are the most accurate previous data. It should be noted that our method gives an exact result for a particular sample at zero temperature and does not require extrapolating from finite temperatures as Monte Carlo data does. The only other exact ground-state calculation for large samples is that of Bieche et al.[30] who use a graph-theoretical method.

VII. EXTENDED AND LOCALIZED STATES

The transition temperature for ferromagnetic ordering decreases from its perfect lattice value at $p = 0$ and goes to zero for p around 12–15 %. We made the observation in an earlier paper[22] that all of the defect eigenstates in our formalism are localized for $p < p_c$ and that, for $p > p_c$, some are extended. These earlier observations were qualitative. The purpose of this and the next section is to put this on a more quantitative basis and to explore some of the consequences.

It is necessary first to have a definition of the spatial extent of an eigenstate. Eigenstates, it will be remembered, occur in pairs $\pm \epsilon$, and the corresponding eigenvectors are complex conjugates of each other and can be written $|p\rangle \pm i|q\rangle$. By way of example, in the simplest singe-defect configuration in Fig. 2, $|p\rangle$ would be localized on one of the frustrated plaquettes and $|q\rangle$ on the other. The "centers of mass" of $|p\rangle$ and $|q\rangle$ are separated by one lattice spacing, and this is a sensible definition of the size of this pair of states. The (Manhattan) distance between the centers of mass of $|p\rangle$ and $|q\rangle$ will be taken generally as the definition of the spatial extent of an eigenstate.

The definition of extended or localized needs to be made more precise. A distribution function N_l is introduced such that N_l is the number of states whose size is larger than l. For a sample of size $L_1 \times L_2$ we might expect, in the large-l limit, distributions of the form

$$N_l = A L_1 L_2 \exp(-l/\xi) \qquad (7.1)$$

or

$$N_l = B L_1 L_2 l^{-\rho} , \qquad (7.2)$$

where A and B are constants and ξ is a characteristic length. A distribution contains significant extended states if it is of the form of Eq. (7.2) with $\rho < 2$; in this case, in a square sample of side L, the number of states whose size is $O(L)$ or greater will approach infinity as $L \to \infty$. If the distribution has $\rho > 2$ or is of the form of Eq. (7.1), then the number of states of size $O(L)$ or greater approaches zero in the limit of an infinite sample. This will be our criterion for determining whether there are localized or extended states present. It should be noted, of course, that the two equations do not take account of finite-size effects and we should interpret the behavior
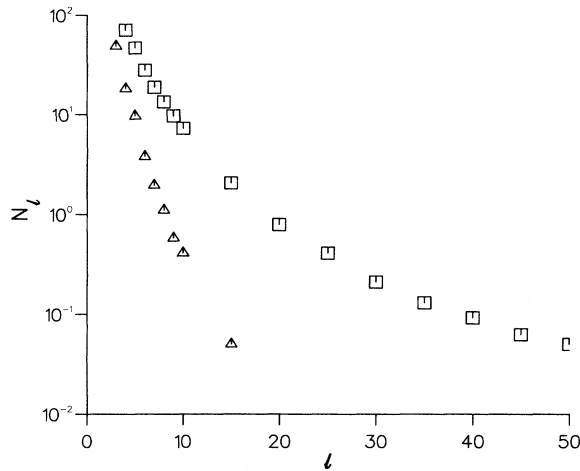
FIG. 9. Distribution N_l (normalized to a 128^2 sample size) as a function of size l for $p = 5\%$ (triangles) and $p = 8\%$ (squares) as a log-linear plot. N_l is averaged over 40 samples sized 32×1024 and 64×512 for the $p = 5\%$ case and over 50 samples sized 128×128 and 128×256 for $p = 8\%$. l is in units of lattice spacings.

with care when l becomes of the order of L_1 or L_2.

Consider first the regime in which $p < p_c$, and the states are expected to be localized. The eigenstates were calculated for a number of samples of width L_2 and length L_1. At $p = 5\%$, no finite size effects were apparent if L_2 was larger than about 32 and, for $p = 8\%$, size effects were similarly absent for L_2 larger than about 64. N_l was calculated and averaged over 40 samples (of sizes 512×64 and 1024×32) for the 5% concentration of defects. At $p = 8\%$ the average was taken over 50 samples (of sizes 128×128 and 128×256). The results are shown in Figs. 9 and 10 on log-linear and bilogarithmic plots, re-

spectively. N_l has been normalized to the value for a 128^2 lattice. It is very clear that the behavior is described well by Eq. (7.2). Using a least-squares fit to the region of the curves in Fig. 10 that are reasonable straight lines we obtain values of the exponent appearing in this equation. They are, for $p = 5\%$, $\rho = 4.73 \pm 0.22$ and, for $p = 8\%$, $\rho = 3.12 \pm 0.08$. In both cases $\rho > 2$, which accords with our criterion for localized states. It will also be noticed that ρ decreases with increasing p.

VIII. CORRELATION FUNCTIONS AT $p = 50\%$

For $p > p_c$, it is anticipated that Eq. (7.2) will still apply but that the exponent ρ will be smaller and there will be a significant number of more extended states. Finite size effects are likely to be unavoidable. We concentrate our attention here on the $p = 50\%$ case which is a canonical spin-glass model. We calculated the eigenstates for six different-size lattices and, in each case, averaged N_l over 80 samples. N_l is plotted against l in Figs. 11–13. We have again normalized N_l to a 128^2-site lattice. The plots indicate that, for l above about 30, Eq. (7.2) represents N_l fairly well. There are two finite size effects. Referring to Fig. 11, which displays the data for square lattices, a drop in N_l is apparent when l becomes comparable to the linear dimension L of the lattice. Since we measure size as a Manhattan distance, clearly N_l must be zero for l larger than $2L$ anyway.

There is a straight-line fit to data points in Fig. 11 over a somewhat limited range of l; a larger sample length than was possible for a square lattice was obviously needed and so calculations were performed on strips. In Fig. 12 the results for strips of length $L_1 = 256$ and two widths L_2 are plotted. The straight line now extends to larger values of l close to 200 lattice spacings.

Finally, we show in Fig. 13 the results for strips of length $L_1 = 512$. For the wider strip with $L_2 = 32$, there

FIG. 10. As Fig. 9 on a bilogarithmic plot.
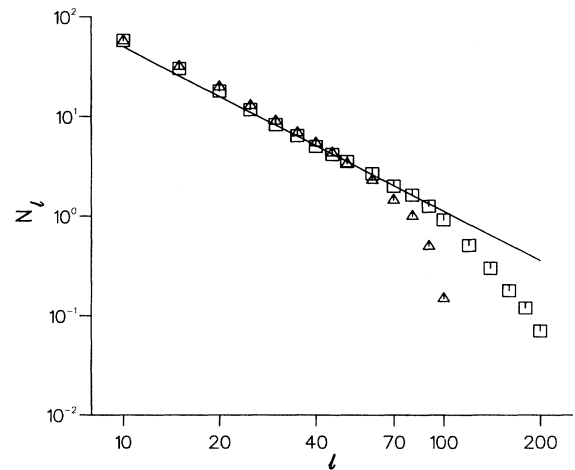
FIG. 11. Distribution N_l (normalized to a 128^2 sample size) as a function of size l for a 64×64 (triangles) and a 128×128 (squares) lattice. $p = 50\%$ and N_l is averaged over 80 samples. l is in units of lattice spacings.
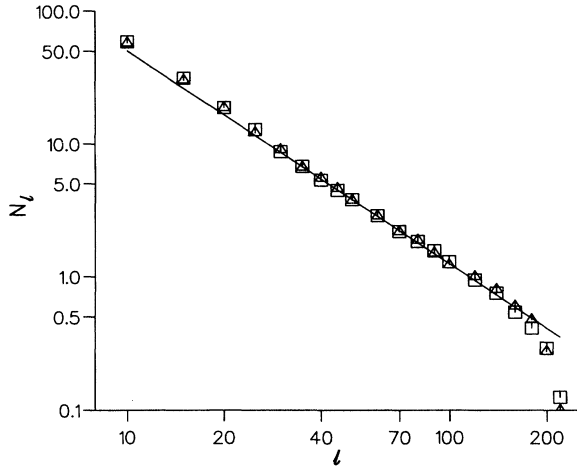
FIG. 12. As Fig. 11 for 256×32 (triangles) and 256×64 (squares) lattices.

is a good agreement with Eq. (7.2) out to $l \simeq 350$ and with the data in the previous figure. More serious finite size effects occur for the narrower strip with $L_2 = 16$. The narrow width is the cause of an overestimate in the value of N_l for intermediate l in contrast to the reduction in N_l at high l that arises from the finite overall size.

The straight lines in the diagrams were obtained by least-squares fits to data points between $l = 30$ and the maximum for which finite size effects are negligible. We obtain a value for the exponent in Eq. (7.2) of $\rho = 1.65 \pm 0.05$ from Fig. 11, $\rho = 1.60 \pm 0.08$ from Fig. 12, and, from Fig. 13, $\rho = 1.57 \pm 0.11$, which are consistent with the criterion $\rho < 2$ for the presence of extended states. In each case the wider sample was the one on which the fit was made. We take Fig. 12 as giving the
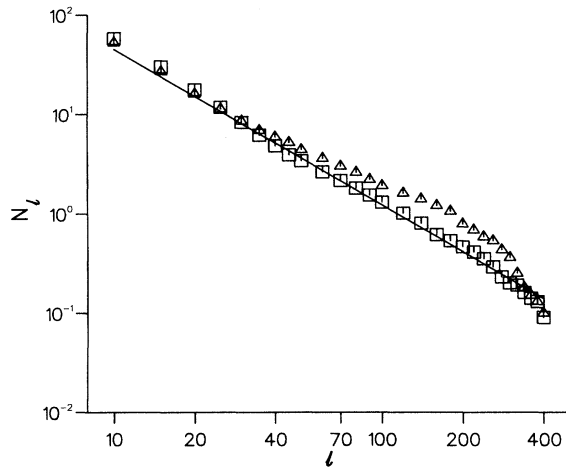
best estimate for ρ, providing as it does a compromise between the small overall size of the Fig. 11 samples and the narrow width of those of Fig. 13. Thus

$$\rho = 1.60 \pm 0.08 \ . \tag{8.1}$$

To aid our thoughts in assessing the consequences of the presence of these extended states, let us consider the simple defect configuration in a perfect lattice shown in Fig. 14. The presence of a row of bonds $-J'$ of length l will produce a defect eigenstate $\epsilon = \pm \frac{1}{2} \exp(-2lJ'/kT)$ of spatial extent l. The extended states we are considering have eigenvalues given by $\epsilon = \pm(X/2)\exp(-2rJ/kT)$, with r of a fairly modest size; it is seldom more than about 10. These eigenstates, therefore, are in some sense analogous to the chain of defects in Fig. 14 with $J' = rJ/l$. Since r is relatively small and $l \to \infty$, this is equivalent to an infinite chain of infinitesimally weak bonds across which, or course, all correlations will vanish.

Now, it must be emphasized that we are not saying that, in this highly disordered regime at $p = 50\%$, any aspect of the frustrated system is equivalent to the configuration in Fig. 14. We are merely using the observation from Fig. 14 to draw the inference that states of size $l \to \infty$ with r finite can reasonably be expected to lead to a loss in correlations between spins.

Let us now consider the spin-spin correlation function in more detail. For the $\pm J$ model in two dimensions, in the regime $p > p_c$ where $T_c = 0$, one assumes that the correlation function at zero temperature takes the form

$$[\langle S_0 S_R \rangle^2]_{\mathrm{av}} = CR^{-\eta} \ , \tag{8.2}$$

where C is a constant and the average is taken over configurations of the system. The spin-glass susceptibility is defined as

$$\chi_{\mathrm{SG}} = \frac{1}{N} \left[\sum_{ij} \langle S_i S_j \rangle^2 \right]_{\mathrm{av}} , \tag{8.3}$$

which, from (8.2), leads to the finite size scaling form, for a system of linear dimension L,

$$\chi_{\mathrm{SG}}(L) \sim L^{2-\eta} \ . \tag{8.4}$$

We can deduce a value for η from the scaling behavior of the extended states of our formalism. Consider a sample of linear dimension L. The number of states whose size is

FIG. 13. As Fig. 11 for 512×16 (triangles) and 512×32 (squares) lattices.
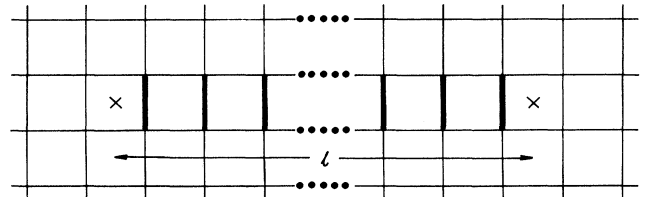
FIG. 14. A defect configuration in an otherwise perfect lattice: a row of l bonds of strength $-J'$ (denoted by heavy lines).

of the order of L scales, from (7.2), as $N_L \sim L^{2-p}$. Now, as stated earlier, the extended states destroy the correlations, and so spins will be correlated within an area whose size scales as L^2/N_L; that is, as L^p.

Now consider the double summation over sites in (8.3). For an arbitrary site i, there are, on average $\sim L^p$ sites j within the region of correlation. Thus $\chi_{SG}(L) \sim L^p$, which, by comparison with (8.4), leads to the following relation between exponents:

$$\eta = 2 - p . \tag{8.5}$$

From the p of Eq. (8.1), we obtain the value $\eta = 0.40 \pm 0.08$. Interestingly, this agrees with Morgenstern and co-workers[5,31] who get $\eta = 0.4 \pm 0.1$, and is in disagreement with the more recent calculations of Bray and Moore[33] who obtain $\eta = 0.20 \pm 0.02$, Wang and Swendsen[34] with $\eta = 0.2$ and Bhatt and Young[35] with $\eta = 0.20 \pm 0.05$. McMillan[32] obtained $\eta = 0.28 \pm 0.04$.

It is useful to examine (8.5) for some limiting cases. If $\eta = 0$, χ_{SG} scales with the size L^2 of the sample [see Eq. (8.4)]. The corresponding value of p, namely 2, implies that spins are correlated over an area $\sim L^2$ also, and the summation over j in (8.3) is over essentially all sites in the system. If $\eta = 2$, then $\chi_{SG} \sim$ constant. A corresponding value for p of zero means that the size of the correlated regions are independent of L and so the number of sites involved in the j summation does not depend on the sample size. Thus Eq. (8.5) expresses consistency in both limits.

A comment is needed about the disagreement between our value of η, namely 0.4, and the value 0.2 that appears in most of the recent very careful calculations.[33,34,35] No firm conclusions about the value of η can be drawn from experimental observations. Measurements[36] on a two-dimensional $\pm J$ system yield values for the exponents: $\gamma = 4.5 \pm 0.2$, $\nu = 2.4 \pm 0.3$; using the scaling relation $\gamma = (2 - \eta)\nu$ and assuming η is nonnegative, gives a value $\eta = 0.2 \pm 0.2$, and all calculations are within that experimental error.

The relation (8.5) is, of course, obtained by inference rather than by direct proof, but it appears to be consistent in the two limits ($p = 0$, $\eta = 2$) and ($p = 2$, $\eta = 0$). The feature that is unique about the present method is that it is actually a zero-temperature calculation rather than an extrapolation from finite temperatures. Also, there are no problems of the sort that occur in Monte Carlo calculations with long relaxation times. A possible source of discrepancy could arise in calculations that use small samples. From Figs. 11–13 it can be seen that N_l falls faster with l for values of l less than about 40 lattice spacings. For calculations on such samples, we might expect values of p larger than we obtain here with corresponding smaller estimates of η.

We have indicated that there is a critical value for p, namely, $p_c = 2$. For the concentrations considered, we have seen that $p < p_c$ if $p > p_c$ and $p > p_c$ if $p < p_c$. It is reasonable to infer that $p = p_c$ at $p = p_c$, and that p_c is determined by a transition from localized to extended states. It also leads us to deduce that the exponent η reduces from the value 0.4 at $p = 50\%$ to zero at $p = p_c$.

As far as we are aware, the p dependence of η has not been investigated by other authors. A related issue is the "random antiphase state" described by Barahona et al.[37] This may be a real phase of the system or simply an artifact of a numerical calculation in the hard-to-access regime where p is near p_c; here, the extended states we have been discussing are incipient or sparse and a controlled analysis of correlations is likely to be a difficult task. We will explore these issues elsewhere.

IX. CONCLUSION

The development of a mean-field description of spin glasses was clearly established a number of years ago.[38,39,16] For short-range systems, the essence of a formalism did appear[1-4] at around the same time, but it did not develop into a useful language. Rather, the advances from short-range systems have been through numerical calculations and, more recently, by means of scaling arguments applied to domain interface energies. The present approach relates in spirit more closely to the work of the late 1970's[1-4] that attempted to exploit the gauge-invariant features of the frustrated system but, in terms of detailed formalism, it is, of course, based on the early reformulations[19,20] of the Onsager theory of the pure Ising model. In modern terms one would use the language of a fermionic field theory expressed in Lagrangian form through an integral over Grassmann variables.[26,40] The availability of a fermion theory in which to reexpress the present work is important because it provides the potential to go beyond two dimensions.

One of the intriguing features of the present formalism is the way in which it emphasizes the fact that frustration really is a special type of disorder. It is so special, in fact, that distinct fermion fields—we now use the modern language—are needed to describe it and, in the zero-temperature ground state, the frustrated and nonfrustrated fermions are completely separable. At finite temperatures there is mixing of the two types of fermions although it is still a free-fermion system.

An important aspect of the theory is the retention of only its gauge-invariant features. Neither the actual position of negative bonds nor a catalogue of ground-state spin configurations is relevant to the thermodynamics of the model and these are absent from the treatment. The gauge-invariant properties stem from the distribution of frustrated plaquettes in the lattice. The number of fermions associated with the frustration is exactly equal to the number of frustrated plaquettes; this is a property which we wish to highlight because it gives the current method a claim to be one based on the minimum information necessary to treat a frustrated system. As far as we are aware, the special features of the frustrated fermions have not been explored by previous authors, although there are echoes of these ideas in the work of Kadanoff and Ceva,[41] which predates the interest in spin glasses.

Extensive numerical calculations, based on the formalism, have been reported in the paper. It is perhaps true to say that, for some of the results, their significance is

more a demonstration of the use of the formalism than something inherently new in itself. This is certainly correct as far as the ground-state energy and entropy calculations are concerned although claims for the precision of the values obtained are made. The inference of a sort of Anderson transition at the critical concentration p_c together with the introduction of a new exponent ρ does provide, however, a quite new insight into the underlying physics that occurs as the frustration in the system is increased. This new development is given precision by relating ρ to the exponent η in the Ising model and identifying the physical significance of a critical p_c.

The question arises as to the possibility of developing this work to provide a more general account of frustrated systems—or at least of the static properties of frustrated Ising systems. We have chosen to examine the two-dimensional $\pm J$ model here. Certainly there is nothing in principle to prevent us examining alternatives to the $\pm J$ model in two dimensions such as that with a Gaussian distribution of bonds. The problem is basically just one of matrix diagonalization even at finite temperatures. The use of perturbation theory to give exact numerical results on large samples is special to this case, however, and would not be easy to adapt for the Gaussian model.

Of more interest is the possibility of extending the ideas to three dimensions. Again, in principle, there are possibilities for doing this, but it is necessary to use a fermion formalism[40] and, rather than free fermions, we have an interacting field theory. Still, there is an interesting prospect. In the ground state, at zero temperature, the interaction term vanishes, and we can obtain the frustrated fermion basis by inspection just as we could in two dimensions; we have merely to identify the frustrated (two-dimensional) plaquettes. To determine the underlying physics at $T=0$, we need to examine the effect of the interaction term at small finite temperatures when it occurs as a small perturbation. The fact that it is a small perturbation provides the intriguing possibility that the low-temperature physics of the $3D$ Ising spin glass may be more amenable to theory than the pure $3D$ Ising system at its critical temperature; in the latter case the interaction term is certainly not a small perturbation. Work is in progress on this and developments will be reported in due course.

APPENDIX: THE CONTINUUM GREEN'S FUNCTION

The Green's function for the continuum states (at $T=0$ and $\epsilon=0$) is defined by

$$G_c = -\sum_c |c\rangle \epsilon_c^{-1} \langle c| , \qquad (A1)$$

so that the full Green's function [see Eq. (4.3)] is

$$G = G_c + \epsilon^{-1} \sum_d |d\rangle\langle d| + O(\epsilon) . \qquad (A2)$$

From the T-matrix expansion, $G = g + gTg$, we can use Eqs. (3.12) and (3.18) to write

$$G = g_0 + \epsilon^{-1} \sum_f g_0|f\rangle\langle f|g_0 + g_0 S g_0 - \sum_f g_0^2|f\rangle\langle f|g_0$$
$$- \sum_f g_0|f\rangle\langle f|g_0^2 + O(\epsilon) . \qquad (A3)$$

Since it can be shown that

$$\sum_f g_0|f\rangle\langle f|g_0 = \sum_d |d\rangle\langle d| , \qquad (A4)$$

we can obtain from Eqs. (A2) and (A3) the following expression for G_c:

$$G_c = g_0 + g_0 S g_0 - g_0 P - P g_0 , \qquad (A5)$$

where

$$P = \sum_d |d\rangle\langle d| . \qquad (A6)$$

Now, using Eqs. (3.16), (3.17), and (A4), we obtain finally for the continuum Green's function

$$G_c = (1-P)g_c(1-P) , \qquad (A7)$$

where

$$g_c = g_0 + g_0 U g_0 . \qquad (A8)$$

[1]G. Toulouse, Commun. Phys. **2**, 115 (1977).
[2]E. Fradkin, B. A. Huberman, and S. H. Shenker, Phys. Rev. B **18**, 4789 (1978).
[3]J. B. Kogut, Rev. Mod. Phys. **51**, 659 (1979).
[4]H. G. Schuster, Z. Phys. B **35**, 163 (1979).
[5]I. Morgenstern and K. Binder, Phys. Rev. B **22**, 288 (1980).
[6]H.-F. Cheung and W. L. McMillan, J. Phys. C **16**, 7027 (1983).
[7]R. N. Bhatt and A. P. Young, Phys. Rev. Lett. **54**, 924 (1985).
[8]A. T. Ogielski and I. Morgenstern, Phys. Rev. Lett. **54**, 928 (1985).
[9]J.-S. Wang and R. H. Swendsen, Phys. Rev. B **38**, 4840 (1988).
[10]J. R. Banavar and M. Cieplak, Phys. Rev. B **26**, 2662 (1982).
[11]W. L. McMillan, Phys. Rev. B **29**, 4026 (1984); **31**, 340 (1985).
[12]A. J. Bray and M. A. Moore, Phys. Rev. B **31**, 631 (1985).
[13]D. L. Stein, G. Baskaran, S. Liang, and M. N. Barber, Phys. Rev. B **36**, 5567 (1987).

[14]D. S. Fisher and D. A. Huse, Phys. Rev. B **38**, 386 (1988).
[15]D. S. Fisher and D. A. Huse, Phys. Rev. B **38**, 373 (1988).
[16]K. Binder and A. P. Young, Rev. Mod. Phys. **58**, 801 (1986).
[17]*Heidelberg Colloquium on Glassy Dynamics,* edited by J. L. Van Hemmen and I. Morgenstern, Lecture Notes in Physics, Vol. 275 (Springer-Verlag, Berlin, 1987).
[18]A. P. Young, in *Disorder in Condensed Matter Physics,* edited by J. A. Blackman and J. Tagüeña (Clarendon, Oxford, 1991), p. 331.
[19]M. Kac and J. C. Ward, Phys. Rev. **88**, 1332 (1952).
[20]H. S. Green and C. A. Hurst, *Order-Disorder Phenomena* (Interscience, London, 1964).
[21]J. A. Blackman, Phys. Rev. B **26**, 4987 (1982).
[22]J. Poulter and J. A. Blackman, J. Phys. C **19**, 569 (1986).
[23]J. A. Blackman and J. Poulter, J. Phys. (Paris) Colloq. **49**, C8-1033 (1988).

[24]J. A. Blackman and J. Poulter, J. Phys. C 17, 107 (1984); 17, 1085 (1984).

[25]S. Samuel, J. Math. Phys. 21, 2806 (1980).

[26]C. Itzykson, Nucl. Phys. B 210, [FS6], 448 (1982).

[27]A. P. Young and R. B. Stinchcombe, J. Phys. C 9, 4419 (1976).

[28]S. Kirkpatrick, Phys. Rev. B 16, 4630 (1977).

[29]J. Vannimenus and G. Toulouse, J. Phys. C 10, L537 (1977).

[30]I. Bieche, R. Maynard, R. Rammal, and J. P. Uhry, J. Phys. A 13, 2553 (1980).

[31]I. Morgenstern and H. Horner, Phys. Rev. B 25, 504 (1982).

[32]W. L. McMillan, Phys. Rev. B 28, 5216 (1983).

[33]A. J. Bray and M. A. Moore, in *Heidelberg Colloquium on Glassy Dynamics* (Ref. 17), p. 121.

[34]J.-S. Wang and R. H. Swendsen, Phys. Rev. B 37, 7745 (1988).

[35]R. N. Bhatt and A. P. Young, Phys. Rev. B 37, 5606 (1988).

[36]C. Dekker, A. F. M. Arts, and H. W. J. de Wijn, Phys. Rev. B 38, 8985 (1988).

[37]F. Barahona, R. Maynard, R. Rammal, and J. P. Uhry, J. Phys. A 15, 673 (1982).

[38]D. Sherrington and S. Kirkpatrick, Phys. Rev. Lett. 35, 1972 (1975).

[39]G. Parisi, Phys. Rev. Lett. 43, 1754 (1979).

[40]C. Itzykson, Nucl. Phys. B 210[FS6], 477 (1982).

[41]L. P. Kadanoff and H. Ceva, Phys. Rev. B 3, 3918 (1971).